

# Optimal Weighting Scheme in Redshift-space Power Spectrum Analysis and a Prospect for Measuring the Cosmic Equation of State

Kazuhiro Yamamoto

*Max-Planck-Institute for Astrophysics, Karl-Schwarzschild-Str. 1, D-85741 Garching,  
Germany*

*Department of Physical Science, Hiroshima University, Higashi-Hiroshima, 739-8526,  
Japan*

kazuhiro@hiroshima-u.ac.jp

## ABSTRACT

We develop a useful formula for power spectrum analysis for high and intermediate redshift galaxy samples, as an extension of the work by Feldman, Kaiser & Peacock (1994). An optimal weight factor, which minimizes the errors of the power spectrum estimator, is obtained so that the light-cone effect and redshift-space distortions are incorporated. Using this formula, we assess the feasibility of the power spectrum analysis with the luminous red galaxy (LRG) sample in the Sloan Digital Sky Survey as a probe of the equation of state of the dark energy. Fisher matrix analysis shows that the LRG sample can be sensitive to the equation of state around redshift  $z=0.13$ . It is also demonstrated that the LRG sample can constrain the equation of state with (1-sigma) error of 10% level, if other fundamental cosmological parameters are well determined independently. For the useful constraint, we point out the importance of modeling the bias taking the luminosity dependence into account. We also discuss the optimized strategy to constrain the equation of state using power spectrum analysis. For a sample with fixed total number of objects, it is most advantageous to have the sample with the mean number density  $10^{-4} h^3 \text{Mpc}^{-3}$  in the range of the redshift  $0.4 \lesssim z \lesssim 1$ .

*Subject headings:* cosmology : theory — galaxies: clusters: general — large scale structure of universe

## 1. INTRODUCTION

The clustering of the cosmological objects like galaxies, clusters of galaxies and QSOs, is the fundamental to probe the Universe because it directly reflects properties of dark components and the primordial density fluctuations. The power spectrum is a simple but very useful tool to characterize their spatial distribution. Actually, useful constraints on the cosmological parameters are obtained from the power spectrum analyses of the Two Degree Field (2df) Galaxy Redshift Survey (Percival et al. 2001) and the 2df QSO Redshift Survey (Hoyle et al. 2002). In such power spectrum analyses, many authors base their methods on the seminal paper by Feldman, Kaiser & Peacock (1994, Hereafter FKP).

For redshift surveys such as the 2df survey and the Sloan Digital Sky Survey (SDSS), however, several observational effects on the power spectrum analysis can be very important. Because cosmological observations are feasible only on the light-cone hypersurface defined by the current observer, the effect of the redshift evolution of the luminosity function, the clustering amplitude, and the bias, contaminates the observational data. We call this the light-cone effect (Matarrese et al. 1997; Matsubara, Suto & Szapudi 1997; de Laix & Starkman 1998; Yamamoto & Suto 1999). On the other hand it is well known that the distribution of the sources in redshift space is different from that in the real space due to the redshift-space distortions. The linear redshift distortion is the effect of the bulk motion of the sources within the linear theory of density perturbation (Kaiser 1987; Hamilton 1998 and references therein). The finger-of-God effect is the redshift distortion due to the random motion of the sources in the nonlinear regime (Mo, Jing & Boerner 1997; Magira, Jing & Suto 2000). The geometric distortion is the effect caused by a choice of the distance-redshift relation to plot a map of the sources (Ballinger, Peacock & Heavens 1996; Matsubara & Suto 1996).

The LRG sample of the SDSS spectroscopic survey will provide a sample of  $10^5$  intrinsically luminous early-type galaxies to  $z \sim 0.5$  (Eisenstein et al. 2001). In the analysis of clustering statistics of such a sample, the light-cone effect and the redshift-space distortions can be substantial. Fortunately these observational effects have been well investigated and we can model the power spectrum incorporating them (see section 3.1). The primary purpose of the present paper is to extend the formulas in FKP in order to incorporate these observational effects and to derive a generalized expression of the optimal weight factor in the power spectrum analysis (cf. Tegmark 1995).

The results of the 2df galaxy survey (Peacock et al. 2001), weak lensing surveys (Refregier et al. 2002; Bacon et al. 2002; and references therein), cosmic microwave background anisotropy measurements (e.g., Ruhl et al. 2002) and type Ia supernovae measurements (Perlmutter et al. 1999; Riess et al. 1998), support the concordance model (Wang et al. 2000): A spatially flat universe dominated by the dark energy component and, with respect

to structure formation, cold dark matter with the primordial density fluctuations predicted in the inflationary scenario. The very recent result by the Wilkinson Microwave Anisotropy Probe (WMAP) strongly supports the concordance model (Spergel et al. 2003). Now the mystery of the dark energy component has become one of the most important issues in cosmology, which has led to recent activity in investigating the dark energy (See e.g. Peebles & Ratra 2003, for a recent review, and references therein). The dark energy can be characterized by its equation of state  $w_X = p_X/\rho_X$ , where  $p_X$  is the pressure and  $\rho_X$  is the energy density. For the cosmological constant,  $w_X = -1$ . However, if the dark energy originates from the vacuum energy of a variable scalar field, like the quintessence model,  $w_X$  can take values  $w_X > -1$ , and can in general be a function of redshift. Thus constraints on the equation of state is quite important in considering the origin of the dark energy. Then various strategies for probing the equation of state have been investigated (e.g. Newman & Davis 2000, Saini, et al. 2000, Wang, et al. 2000, Chiba & Nakamura 2000, Huterer & Turner 2001, Yamamoto & Nishioka 2001, Kujat et al. 2002, and references therein).

Second purpose of this paper is to assess the feasibility of measuring the equation of state using the power spectrum analysis.<sup>1</sup> Recently, Matsubara & Szalay have discussed the usefulness of the LRG sample in SDSS for measuring the cosmological parameters (2002). Their method is based on maximum likelihood analysis in redshift space. They demonstrated the usefulness of various SDSS samples to constrain cosmological parameters by estimating the Fisher matrix element. Motivated by their work, we assess the feasibility of the method with the power spectrum analysis of the LRG sample in SDSS to probe the equation of state based on the Fisher matrix formalism for power spectrum analysis (Tegmark 1997, Tegmark et al. 1998a). The advantage of our method is that the formulae are simple and analytic, which allows us to evaluate the formulae easily and to understand meaning of results clearly.

This paper is organized as follows: In section 2, we derive formulae for the power spectrum analysis taking the light-cone effect and the redshift-space distortions into account. In section 3, the Fisher matrix element is evaluated using an approximate method. There we focus on the matrix elements relevant to a measurement of dark energy, especially the equation of state. In section 4, we discuss optimizing the strategy, for a sample with a fixed total number of objects, using the power spectrum to probe the equation of state. Section 5 is devoted to summary and conclusions. Throughout this paper we use a system of units in which the velocity of light  $c$  equals 1.

---

<sup>1</sup>After completing this work, a similar investigation by Matsubara & Szalay (2003) has been announced.

## 2. FORMALISM

In this section we present an optimal weighting scheme of the power spectrum analysis for redshift surveys taking the redshift-space distortions and the light-cone effect into account. We obtain the generalized optimal weight factor, which minimizes errors of a power spectrum estimator, as a simple extension of the scheme developed by FKP. On the basis of this result, we derive the expression of the Fisher matrix element in subsection 2.2.

In a redshift survey, the redshift  $z$  is the indicator of the distance, therefore, we need to *assume* a distance-redshift relation to plot a map of objects. For this distance, in the present paper, we adopt the following expression, which is the comoving distance in spatially flat universes

$$s(z) = \frac{1}{H_0} \int_0^z \frac{dz'}{\sqrt{\Omega_0(1+z')^3 + 1 - \Omega_0}}, \quad (1)$$

where  $H_0 = 100h\text{km/s/Mpc}$  is the Hubble parameter and we fix  $\Omega_0 = 0.3$ . Our formula presented below is general, and it does not depend on this choice of  $s(z)$ .

### 2.1. Optimal Weight Factor

The derivation of the optimal weight factor in this subsection is essentially same as that of FKP. Some parts of equations here can be found in FKP, which we have not omitted for being self-contained of the present paper. We denote the number density field of sources (real catalog) by  $n_g(\mathbf{s})$ , where  $\mathbf{s}(= s(z)\boldsymbol{\gamma})$  is the three dimensional coordinate in the (cosmological) redshift space and  $\boldsymbol{\gamma}$  is the unit directional vector. We use  $\bar{n}(\mathbf{s})$  to denote the expected mean number density. We define the fluctuation field to be

$$F(\mathbf{s}) = n_g(\mathbf{s}) - \alpha n_s(\mathbf{s}), \quad (2)$$

where  $n_g(\mathbf{s}) = \sum_i \delta(\mathbf{s} - \mathbf{s}_i)$ , with  $\mathbf{s}_i$  being the location of the  $i$ -th object, similarly  $n_s(\mathbf{s})$  is the density of a synthetic catalog which has mean number density  $1/\alpha$  times that of the real catalog. For  $n_g(\mathbf{s})$  and  $n_s(\mathbf{s})$ , following FKP, we assume

$$\langle n_g(\mathbf{s}_1)n_g(\mathbf{s}_2) \rangle = \bar{n}(\mathbf{s}_1)\bar{n}(\mathbf{s}_2)(1 + \xi(\mathbf{s}_1, \mathbf{s}_2)) + \bar{n}(\mathbf{s}_1)\delta(\mathbf{s}_1 - \mathbf{s}_2), \quad (3)$$

$$\langle n_s(\mathbf{s}_1)n_s(\mathbf{s}_2) \rangle = \alpha^{-2}\bar{n}(\mathbf{s}_1)\bar{n}(\mathbf{s}_2) + \alpha^{-1}\bar{n}(\mathbf{s}_1)\delta(\mathbf{s}_1 - \mathbf{s}_2), \quad (4)$$

$$\langle n_g(\mathbf{s}_1)n_s(\mathbf{s}_2) \rangle = \alpha^{-1}\bar{n}(\mathbf{s}_1)\bar{n}(\mathbf{s}_2), \quad (5)$$

where  $\xi(\mathbf{s}_1, \mathbf{s}_2)$  denotes the correlation function.

We define the Fourier coefficient of  $F(\mathbf{s})$ , with a conventional weight factor, to be

$$\mathcal{F}(\mathbf{k}) = \frac{\int ds w(\mathbf{s}, \mathbf{k}) F(\mathbf{s}) e^{i\mathbf{k}\cdot\mathbf{s}}}{[\int ds \bar{n}(\mathbf{s})^2 w(\mathbf{s}, \mathbf{k})^2]^{1/2}}, \quad (6)$$

where  $w(\mathbf{s}, \mathbf{k})$  is the weight function which can be adjusted to optimize the power spectrum estimator below. Then the expectation value of the square  $|\mathcal{F}(\mathbf{k})|^2$  is written,

$$\langle |\mathcal{F}(\mathbf{k})|^2 \rangle = \frac{\int d\mathbf{s}_1 \int d\mathbf{s}_2 w(\mathbf{s}_1, \mathbf{k}) w(\mathbf{s}_2, \mathbf{k}) \langle F(\mathbf{s}_1) F(\mathbf{s}_2) \rangle e^{i\mathbf{k} \cdot (\mathbf{s}_1 - \mathbf{s}_2)}}{\int d\mathbf{s} \bar{n}(\mathbf{s})^2 w(\mathbf{s}, \mathbf{k})^2}. \quad (7)$$

Using equations (3)-(5), we have

$$\langle F(\mathbf{s}_1) F(\mathbf{s}_2) \rangle = \bar{n}(\mathbf{s}_1) \bar{n}(\mathbf{s}_2) \xi(\mathbf{s}_1, \mathbf{s}_2) + (1 + \alpha) \bar{n}(\mathbf{s}_1) \delta(\mathbf{s}_1 - \mathbf{s}_2). \quad (8)$$

Under the distant observer approximation,  $|\mathbf{s}_1 - \mathbf{s}_2| \ll |\mathbf{s}_1|, |\mathbf{s}_2|$ , the correlation function can be expressed as

$$\xi(\mathbf{s}_1, \mathbf{s}_2) = \int \frac{d\tilde{\mathbf{k}}}{(2\pi)^3} P(\tilde{\mathbf{k}}, |\bar{\mathbf{s}}|) e^{-i\tilde{\mathbf{k}} \cdot (\mathbf{s}_1 - \mathbf{s}_2)}, \quad (9)$$

where  $P(\tilde{\mathbf{k}}, |\bar{\mathbf{s}}|)$  is the redshift-space power spectrum at the distance  $|\bar{\mathbf{s}}|$ , where we defined  $\bar{\mathbf{s}} = (\mathbf{s}_1 + \mathbf{s}_2)/2$ . We also adopt the approximation

$$w(\mathbf{s}_1, \mathbf{k}) w(\mathbf{s}_2, \mathbf{k}) \bar{n}(\mathbf{s}_1) \bar{n}(\mathbf{s}_2) \simeq w(\bar{\mathbf{s}}, \mathbf{k})^2 \bar{n}(\bar{\mathbf{s}})^2, \quad (10)$$

which yields

$$\langle |\mathcal{F}(\mathbf{k})|^2 \rangle = \frac{\int d\bar{\mathbf{s}} \bar{n}(\bar{\mathbf{s}})^2 w(\bar{\mathbf{s}}, \mathbf{k})^2 P(\mathbf{k}, |\bar{\mathbf{s}}|) + (1 + \alpha) \int d\mathbf{s} \bar{n}(\mathbf{s}) w(\mathbf{s}, \mathbf{k})^2}{\int d\mathbf{s} \bar{n}(\mathbf{s})^2 w(\mathbf{s}, \mathbf{k})^2}. \quad (11)$$

The last term of the right hand side of equation (11) corresponds to the shot-noise, therefore the estimator of the power spectrum should be defined as

$$\mathcal{P}(\mathbf{k}) = |\mathcal{F}(\mathbf{k})|^2 - P_{\text{shot}}(\mathbf{k}), \quad (12)$$

where  $P_{\text{shot}}$  is defined

$$P_{\text{shot}}(\mathbf{k}) = \frac{(1 + \alpha) \int d\mathbf{s} \bar{n}(\mathbf{s}) w(\mathbf{s}, \mathbf{k})^2}{\int d\mathbf{s} \bar{n}(\mathbf{s})^2 w(\mathbf{s}, \mathbf{k})^2}. \quad (13)$$

The angular average of  $\mathcal{P}(\mathbf{k})$  over a thin shell of the radius  $k (= |\mathbf{k}|)$  in the Fourier space gives the estimator of the angular averaged power spectrum

$$\mathcal{P}_0(k) = \frac{1}{V_k} \int_{V_k} d\mathbf{k} \mathcal{P}(\mathbf{k}), \quad (14)$$

where  $V_k$  denotes the volume of the shell. Thus the expectation value of  $\mathcal{P}_0(k)$  gives the angular averaged power spectrum incorporating the light-cone effect

$$\langle \mathcal{P}_0(k) \rangle = \frac{\int d\mathbf{s} \bar{n}(\mathbf{s})^2 w(\mathbf{s}, \mathbf{k})^2 P_0(k, |\mathbf{s}|)}{\int d\mathbf{s} \bar{n}(\mathbf{s})^2 w(\mathbf{s}, \mathbf{k})^2}, \quad (15)$$

where

$$P_0(k, |\mathbf{s}|) = \frac{1}{V_k} \int_{V_k} d\mathbf{k} P(\mathbf{k}, |\mathbf{s}|). \quad (16)$$

Next we consider the variance of  $\mathcal{P}(\mathbf{k})$ , defined by

$$\begin{aligned} \langle \Delta \mathcal{P}(\mathbf{k}) \Delta \mathcal{P}(\mathbf{k}') \rangle &= \langle [\mathcal{P}(\mathbf{k}) - \langle \mathcal{P}(\mathbf{k}) \rangle] [\mathcal{P}(\mathbf{k}') - \langle \mathcal{P}(\mathbf{k}') \rangle] \rangle \\ &= \langle \mathcal{P}(\mathbf{k}) \mathcal{P}(\mathbf{k}') \rangle - \langle \mathcal{P}(\mathbf{k}) \rangle \langle \mathcal{P}(\mathbf{k}') \rangle, \end{aligned} \quad (17)$$

which is rephrased, by using (12),

$$\langle \Delta \mathcal{P}(\mathbf{k}) \Delta \mathcal{P}(\mathbf{k}') \rangle = \langle |\mathcal{F}(\mathbf{k})|^2 |\mathcal{F}(\mathbf{k}')|^2 \rangle - \langle |\mathcal{F}(\mathbf{k})|^2 \rangle \langle |\mathcal{F}(\mathbf{k}')|^2 \rangle. \quad (18)$$

Substituting (6) into equation (18), we have

$$\begin{aligned} \langle \Delta \mathcal{P}(\mathbf{k}) \Delta \mathcal{P}(\mathbf{k}') \rangle &= \\ &= \frac{2 \prod_{i=1}^2 [\int d\mathbf{s}_i w(\mathbf{s}_i, \mathbf{k})] \prod_{j=3}^4 [\int d\mathbf{s}_j w(\mathbf{s}_j, \mathbf{k}')] \langle F(\mathbf{s}_1) F(\mathbf{s}_3) \rangle \langle F(\mathbf{s}_2) F(\mathbf{s}_4) \rangle e^{i\mathbf{k} \cdot (\mathbf{s}_1 - \mathbf{s}_2)} e^{-i\mathbf{k}' \cdot (\mathbf{s}_3 - \mathbf{s}_4)}}{\left[ \int d\mathbf{s} \bar{n}(\mathbf{s})^2 w(\mathbf{s}, \mathbf{k})^2 \right] \left[ \int d\mathbf{s}' \bar{n}(\mathbf{s}')^2 w(\mathbf{s}', \mathbf{k}')^2 \right]}, \end{aligned} \quad (19)$$

where we assumed the following relation, which is exact when  $F(\mathbf{s})$  follows the statistics of the Gaussian random field,

$$\begin{aligned} \langle F(\mathbf{s}_1) F(\mathbf{s}_2) F(\mathbf{s}_3) F(\mathbf{s}_4) \rangle &= \langle F(\mathbf{s}_1) F(\mathbf{s}_2) \rangle \langle F(\mathbf{s}_3) F(\mathbf{s}_4) \rangle \\ &+ \langle F(\mathbf{s}_1) F(\mathbf{s}_3) \rangle \langle F(\mathbf{s}_2) F(\mathbf{s}_4) \rangle \\ &+ \langle F(\mathbf{s}_1) F(\mathbf{s}_4) \rangle \langle F(\mathbf{s}_3) F(\mathbf{s}_2) \rangle. \end{aligned} \quad (20)$$

In a similar way to derive equation (11), using the distant observer approximation, one can have the relation

$$\begin{aligned} &\int d\mathbf{s}_1 \int d\mathbf{s}_3 w(\mathbf{s}_1, \mathbf{k}) w(\mathbf{s}_3, \mathbf{k}') \langle F(\mathbf{s}_1) F(\mathbf{s}_3) \rangle e^{i\mathbf{k} \cdot \mathbf{s}_1 - i\mathbf{k}' \cdot \mathbf{s}_3} \\ &\simeq \int d\bar{\mathbf{s}} \bar{n}(\bar{\mathbf{s}})^2 w(\bar{\mathbf{s}}, \mathbf{k}) w(\bar{\mathbf{s}}, \mathbf{k}') e^{i\bar{\mathbf{s}} \cdot (\mathbf{k} - \mathbf{k}')} \left[ P\left(\frac{\mathbf{k} + \mathbf{k}'}{2}, |\bar{\mathbf{s}}|\right) + \frac{\alpha + 1}{\bar{n}(\bar{\mathbf{s}})} \right]. \end{aligned} \quad (21)$$

Then, with a repeated use of the distant observer approximation, we have

$$\langle \Delta \mathcal{P}(\mathbf{k}) \Delta \mathcal{P}(\mathbf{k}') \rangle \simeq \frac{2 \int d\bar{\mathbf{s}} \bar{n}(\bar{\mathbf{s}})^4 w(\bar{\mathbf{s}}, \mathbf{k})^4 (P(\mathbf{k}, \bar{\mathbf{s}}) + (1 + \alpha)/\bar{n}(\bar{\mathbf{s}}))^2 (2\pi)^3 \delta^{(3)}(\mathbf{k} - \mathbf{k}')}{[\int d\mathbf{s} \bar{n}(\mathbf{s})^2 w(\mathbf{s}, \mathbf{k})^2]^2}. \quad (22)$$

From (14), the variance of  $\mathcal{P}_0(k)$  is obtained by

$$\begin{aligned} \langle \Delta \mathcal{P}_0(k)^2 \rangle &\equiv \langle [\mathcal{P}_0(k) - \langle \mathcal{P}_0(k) \rangle]^2 \rangle \\ &= \frac{1}{V_k^2} \int_{V_k} d\mathbf{k} \int_{V_k} d\mathbf{k}' \langle \Delta \mathcal{P}(\mathbf{k}) \Delta \mathcal{P}(\mathbf{k}') \rangle, \end{aligned} \quad (23)$$

which reduces to

$$\langle \Delta \mathcal{P}_0(k)^2 \rangle = 2 \frac{(2\pi)^3 \int d\bar{\mathbf{s}} \bar{n}(\bar{\mathbf{s}})^4 w(\bar{\mathbf{s}}, \mathbf{k})^4 Q^2(k, \bar{\mathbf{s}})}{V_k [\int d\mathbf{s} \bar{n}(\mathbf{s})^2 w(\mathbf{s}, \mathbf{k})^2]^2}, \quad (24)$$

where we defined

$$Q^2(k, \bar{\mathbf{s}}) = \frac{1}{V_k} \int_{V_k} d\mathbf{k} \left[ P(\mathbf{k}, |\bar{\mathbf{s}}|) + \frac{\alpha + 1}{\bar{n}(\bar{\mathbf{s}})} \right]^2. \quad (25)$$

The optimal weight factor  $w(\mathbf{s}, \mathbf{k})$  which minimizes  $\langle \Delta \mathcal{P}_0(k)^2 \rangle$  is found from the stationary solution against the variation  $w \rightarrow w + \delta w$ , to be

$$w(\mathbf{s}, k) = \frac{1}{\bar{n}(\mathbf{s}) Q(k, \mathbf{s})}. \quad (26)$$

This generalized formula incorporates the redshift distortions. In general, the redshift space power spectrum  $P(\mathbf{k}, s)$  is written, in terms of the multipole expansion,

$$P(\mathbf{k}, s) = \sum_{l=0,2,\dots} P_l(k, s) \mathcal{L}_l(\mu), \quad (27)$$

where  $\mu$  is the directional cosine between the line of sight  $\gamma$  and the wave number vector,  $\mu = \cos(\gamma \cdot \mathbf{k}/k)$ ,  $\mathcal{L}_l(x)$  is the Legendre polynomial of the  $l$ -th order, and  $P_l(k, s)$  are the expansion coefficients. Then (25) reduces to

$$Q^2(k, \bar{\mathbf{s}}) = \left( P_0(k, |\bar{\mathbf{s}}|) + \frac{1}{\bar{n}(\bar{\mathbf{s}})} \right)^2 + P_2(k, |\bar{\mathbf{s}}|)^2 + P_4(k, |\bar{\mathbf{s}}|)^2 + \dots, \quad (28)$$

where we considered the limit  $\alpha \ll 1$ . In practice, the contribution of higher moments  $l \geq 2$  is not large (cf. Yamamoto 2003). Neglecting this higher moments and the redshift dependence of the power spectrum, (26) reduces to the similar expression by FKP (cf. Peebles 1980),

$$w(\mathbf{s}, k) \simeq \frac{1}{1 + \bar{n}(\mathbf{s}) P_0(k, |\mathbf{s}|)}, \quad (29)$$

then, from equation (24), we have

$$\langle \Delta \mathcal{P}_0(k)^2 \rangle = 2 \frac{(2\pi)^3}{V_k} \left[ \int d\mathbf{s} \frac{\bar{n}(\mathbf{s})^2}{(1 + \bar{n}(\mathbf{s})P_0(k, |\mathbf{s}|))^2} \right]^{-1}. \quad (30)$$

Here we mention a technical problem of the above optimal weight factor. Namely, this weight factor contains the power spectrum at each redshift, i.e.  $P_0(k, s[z])$ . It might be difficult to evaluate it with a sufficient accuracy from a observational data set. A possible alternation is to adopt the weight factor:

$$w(\mathbf{s}, k) = \frac{1}{1 + \bar{n}(\mathbf{s})\langle \mathcal{P}_0(k) \rangle}. \quad (31)$$

This modified weight factor does not minimize the errors, however, it might be useful in a realistic situation of data analysis. The weight factor contains  $\langle \mathcal{P}_0(k) \rangle$ , then it must be solved with equation (15) as a coupled system. However, we can easily solve the coupled equation numerically by iterations. In this case the amplitude of the covariance matrix  $\langle \Delta \mathcal{P}_0(k)^2 \rangle$  is different from the expression (30). It is obtained by substituting (31) into (24), but the expression is rather complicated than (30). As we show below, the use of the modified weight factor alters the expression of the Fisher matrix element. However, the difference is not significant. For example, the use of the modified weight factor increases the  $1 - \sigma$  error of the equation of state  $\Delta \bar{w}$  (see below) by 10 % level. Then our conclusion does not depend on the choice of the above weight factors.

## 2.2. Fisher Matrix Element

In order to estimate the accuracy to which we can constrain cosmological parameters with a measurement of the power spectrum, we employ the Fisher matrix approach. With the Fisher-matrix analysis, one can estimate the best statistical errors on parameters from a given data set (Kendall & Stuart 1969). For this reason, this approach is widely used to estimate how accurately cosmological parameters are determined from large surveys, such as the large scale structure of galaxies, cosmic microwave background anisotropy measurement and supernova data sets. (See e.g. Tegmark, Taylor, & Heavens 1997, Jungman et al. 1996a, 1996b, Zaroubi et al. 1995, Fisher et al. 1995, Tegmark et al. 1998b). In general, the Fisher matrix is defined by

$$F_{ij} = - \left\langle \frac{\partial^2 \ln L}{\partial \theta_i \partial \theta_j} \right\rangle, \quad (32)$$

where  $L$  is the probability distribution function of a data set, given model parameters  $\theta_i$ . For a measurement of galaxy power spectrum, the Fisher matrix is presented using a suitable

approximation in the references (Tegmark 1997, Tegmark et al. 1998a). Here we briefly review a derivation of the Fisher matrix: For simplicity, we adopt the approximation of the Gaussian probability distribution function for  $\Delta\mathcal{P}(\mathbf{k})$ ,

$$L \propto \exp \left[ -\frac{1}{2} \int d\mathbf{k} \int d\mathbf{k}' \Delta\mathcal{P}(\mathbf{k}) C(\mathbf{k}, \mathbf{k}') \Delta\mathcal{P}(\mathbf{k}') \right], \quad (33)$$

where  $C(\mathbf{k}, \mathbf{k}')$  is the inverse matrix of the covariance matrix  $\langle \Delta\mathcal{P}(\mathbf{k}) \Delta\mathcal{P}(\mathbf{k}') \rangle$ . Then, using (25), we have

$$F_{ij} \simeq \frac{1}{4\pi^2} \int_{k_{\min}}^{k_{\max}} \kappa(k) \frac{\partial \langle \mathcal{P}_0(k) \rangle}{\partial \theta_i} \frac{\partial \langle \mathcal{P}_0(k) \rangle}{\partial \theta_j} k^3 d \ln k, \quad (34)$$

where  $\kappa(k)$  is

$$\kappa(k)^{-1} = \frac{\int d\bar{\mathbf{s}} \bar{n}(\bar{\mathbf{s}})^4 w(\bar{\mathbf{s}}, k)^4 (P_0(k, \bar{\mathbf{s}}) + 1/\bar{n}(\bar{\mathbf{s}}))^2}{[\int d\mathbf{s} \bar{n}(\mathbf{s})^2 w(\mathbf{s}, k)^2]^2}, \quad (35)$$

and  $\langle \mathcal{P}_0(k) \rangle$  is the expectation value of the power spectrum, i.e. expression (15). The Fisher matrix depends on the weight factor, and we have

$$\kappa(k) = \Delta\Omega \int d\mathbf{s} s^2 \frac{\bar{n}(s)^2}{(1 + \bar{n}(s)P_0(k, s))^2} \quad (36)$$

for the optimal weight factor (29), and

$$\kappa(k) = \frac{\Delta\Omega [\int d\mathbf{s} s^2 \bar{n}(s)^2 (1 + \bar{n}(s) \langle \mathcal{P}_0(k) \rangle)^{-2}]^2}{\int d\mathbf{s} s^2 \bar{n}(s)^4 (P_0(k, s) + 1/\bar{n}(s))^2 (1 + \bar{n}(s) \langle \mathcal{P}_0(k) \rangle)^{-4}} \quad (37)$$

for the modified weight factor (31), respectively, where we assumed that the mean number density is a function of the distance  $s(=|\mathbf{s}|)$ , and  $\Delta\Omega$  is the survey area. The result is consistent with the previous work: In the limit that the linear redshift distortion, the geometric distortion, and the light-cone effect are switched off, the above results reproduce the previous work (e.g., Tegmark 1997). By using the Bayes theorem, the probability distribution in the parameter space can be written

$$p(\theta_i) \propto \exp \left[ -\frac{1}{2} \sum_{ij} (\theta_i - \theta_i^{\text{tr}}) F_{ij} (\theta_j - \theta_j^{\text{tr}}) \right], \quad (38)$$

where we have assumed that errors in the target model parameters  $\theta_i^{\text{tr}}$  are small. Thus the Fisher matrix gives the uncertainties in the parameter spaces, which are described by a Gaussian distribution function around  $\theta_i^{\text{tr}}$ .

### 3. CONSTRAINTS

In this section we investigate a prospect of the power spectrum analysis of the LRG sample in the SDSS. As pointed out by Matsubara & Szalay (2002), the LRG sample can be a useful tool to constrain the cosmological parameters. Here we assess the potential of the LRG sample to constrain the equation of state of the dark energy. Because the LRG sample is distributed out to a redshift  $\sim 0.5$ , the geometric distortion is substantial. This is the reason why the power spectrum analysis of the LRG sample can constrain the equation of state  $w_X$  even if the original matter power spectrum (or the transfer function) does not depend on  $w_X$ . In comparison to the LRG sample, the SDSS quasars are distributed out to  $z \simeq 5$ , however, the spatial distribution is very sparse. Then the constraint from the quasar sample will not be very tight due to the large shot-noise contribution (Matsubara & Szalay 2002, Yamamoto 2002).

The clustering properties of the LRG sample have not been analyzed so far, then we here assume simple linear bias models for the clustering. (See equation (46) and section 3.3 for a luminosity dependent bias model). To evaluate the Fisher matrix element, the number density of the sample  $\bar{n}(z)$  is an important factor. In the present paper, we adopt the LRG sample with the comoving number density in the reference by Eisenstein et al. (2001, Figure 12 in their paper), as a function of the redshift in the range  $0.2 \leq z \leq 0.55$ . The typical number density of LRGs is  $\bar{n} \simeq 10^{-4} [h^{-1}\text{Mpc}]^{-3}$ . The peak value of the power spectrum is  $10^5 [h^{-1}\text{Mpc}]^3$ . Thus  $\bar{n}(z)P_0(k, z)$  does not exceed 10.

#### 3.1. Modeling the Power Spectrum

We restrict ourselves to a spatially flat universe for modeling the cosmology. This assumption can be justified by the inflationary universe scenario and the recent results of the cosmic microwave anisotropy measurements. We consider a cosmological model with the dark energy component with the equation of state which is variable in time. We assume that the time variation of the equation of state  $w_X(z) = p_X/\rho_X$  is slow. The equation of motion,  $d(\rho_X V(z)) + p_X dV(z) = 0$  with a volume  $V(z) \propto (1+z)^{-3}$ , yields

$$\frac{\rho_X(z)}{\rho_X(z=0)} = (1+z)^3 \exp \left[ 3 \int_0^z \frac{w_X(z')}{1+z'} dz' \right] \equiv f_X(z). \quad (39)$$

With the parameters  $\bar{w}$  and  $\nu$ , we assume  $w_X$  can be parametrized by

$$w_X(z) = \bar{w} \left( \frac{1+z}{1+z_*} \right)^\nu, \quad (40)$$

where  $z_*$  is a constant, then we have

$$f_X(z) = (1+z)^3 \exp \left[ \frac{3\bar{w}}{(1+z_*)^\nu} \left( \frac{(1+z)^\nu - 1}{\nu} \right) \right]. \quad (41)$$

Denoting the matter density parameter by  $\Omega_m$ , the comoving distance is

$$r(z) = \frac{1}{H_0} \int_0^z \frac{dz'}{\sqrt{\Omega_m(1+z')^3 + (1-\Omega_m)f_X(z')}}. \quad (42)$$

We can model the power spectrum in redshift space  $s(z)$  as (Ballinger, Peacock, & Heavens 1996)

$$P_0(k, s(z)) = \frac{1}{c_{\parallel}(z)c_{\perp}(z)^2} \int_0^1 d\mu P_{\text{gal}} \left( q_{\parallel} \rightarrow \frac{k\mu}{c_{\parallel}}, q_{\perp} \rightarrow \frac{k\sqrt{1-\mu^2}}{c_{\perp}}, z \right), \quad (43)$$

where  $P_{\text{gal}}(q_{\parallel}, q_{\perp}, z)$  is the galaxy power spectrum,  $q_{\parallel}$  and  $q_{\perp}$  are the wave number components parallel and perpendicular to the line-of-sight direction in real space with  $r(z)$ , and we define

$$c_{\parallel}(z) = \frac{dr(z)}{ds(z)} \quad \text{and} \quad c_{\perp}(z) = \frac{r(z)}{s(z)}. \quad (44)$$

The geometric distortion is described by scaling the wave number by  $c_{\parallel}(z)$  and  $c_{\perp}(z)$ . Then, even if the original matter power spectrum or the transfer function does not depend on the parameter of the dark energy  $w_X$ , the power spectrum observed in redshift-space can depend on  $w_X$ . Thus we can test the nature of dark energy. This idea traces back to the geometric test pointed out by Alcock & Paczynski (1979). We model the power spectrum in the distribution of galaxy by

$$P_{\text{gal}}(q_{\parallel}, q_{\perp}, z) = \left( 1 + \frac{f(z)}{b(z)} \frac{q_{\parallel}^2}{q^2} \right)^2 b(z)^2 P_{\text{mass}}(q, z), \quad (45)$$

where  $q^2 = q_{\parallel}^2 + q_{\perp}^2$ ,  $b(z)$  is a scale independent bias factor,  $P_{\text{mass}}(q, z)$  is the CDM mass power spectrum, and we defined  $f(z) = d \ln D(z) / d \ln a(z)$  with the linear growth rate  $D(z)$  and the scale factor  $a(z)$ . The term in proportion to  $f(z)$  describes the linear distortion (Kaiser 1987). Following the work by Matsubara & Szalay (2002), we work within the linear theory of density perturbation, adopting the fitting formula of the transfer function by Eisenstein & Hu (1998). Here we consider a simple bias model parametrized by,

$$b(z) = 1 + (b_0 - 1) \frac{1}{D(z)^p}, \quad (46)$$

where  $b_0$  and  $p$  are constants. For  $f(z)$  we adopt the fitting formula developed by Wang and Steinhardt (1998)

$$f(z) \simeq \Omega(z)^{\alpha(w_X)}, \quad (47)$$

with

$$\alpha(w_X) = \frac{3}{5 - w_X/(1 - w_X)} + \frac{3}{125} \frac{(1 - w_X)(1 - 3w_X/2)}{(1 - 6w_X/5)^3} (1 - \Omega(z)), \quad (48)$$

$$\Omega(z) = \frac{\Omega_m}{\Omega_m + (1 - \Omega_m)(1 + z)^{-3} f_X(z)}. \quad (49)$$

In the present paper, we work within the linear theory of density perturbations and we do not consider the nonlinear and the finger of God effects. The nonlinear effect is substantial on small scales in the nonlinear regime (Mo, Jing & Boerner 1997; Magira, Jing & Suto 2000). The inclusion of the nonlinear effect will not alter our result significantly, however, any uncertainty of modeling the nonlinear effect reduces the capability to determine cosmological parameters precisely (cf. Watkins et al. 2002).

### 3.2. Constraints on $w_X$

In our analysis we focus on the sensitivity of the power spectrum analysis on the nature of the dark energy, then we consider the parameters  $(\Omega_m, \bar{w}, \nu, b_0, p)$ . We assume that other cosmological parameters such as the baryon density  $\Omega_b$ ,  $\sigma_8$  and the index of the initial density power spectrum  $n$  are well determined. We might expect to obtain such information in the near future from other observations of the cosmic microwave background anisotropies and the large scale structure of the main galaxy sample in SDSS, etc. Actually the WMAP result have demonstrated the cosmological parameters can be determined from the cosmic microwave background anisotropies. In the present paper, we take  $\Omega_m = 0.28$ ,  $\Omega_b h^2 = 0.024$ ,  $h = 0.7$ ,  $\sigma_8 = 0.9$  and  $n = 1$  (Spergel et al. 2003). On the other hand, the bias is an annoying problem, though the physical mechanism has been extensively investigated (e.g. Mo & White 1996). Recent investigation reports that the bias depends on the luminosity and galaxy type (Norberg et al. 2001, 2002). Thus the bias depends on sample, and it should be determined from the same data simultaneously. In our investigation, we here consider the marginalized probability function integrating over the bias parameters  $b_0$  and  $p$  in (38).

Figure 1 shows the contour of the marginalized probability function on  $\Omega_m - \bar{w}$  space, which is obtained by integrating (38) with respect to  $(\nu, b_0, p)$ . Here, we adopted the target parameters  $(\theta_i^{\text{tr}})$  as follows:  $\Omega_m = 0.28$ ,  $\bar{w} = -1$ ,  $\nu = 0$ ,  $b_0 = 1.5$  and  $p = 1$ . The target parameter of the equation of state corresponds to the cosmological constant. The dependence of the bias modeling is discussed in more detail in section 3.3. In (40), we here set  $z_* = 0.13$ . We also assume the survey area  $10^4 \text{ deg}^2$ , which corresponds to the complete

SDSS sample.<sup>2</sup> We adopted the range of the integration in (34) being  $k_{\min} = 0.001 \text{ hMpc}^{-1}$  and  $k_{\max} = 1 \text{ hMpc}^{-1}$ . Our results do not depend on  $k_{\min}$  as long as  $k_{\min} \lesssim 0.01 \text{ hMpc}^{-1}$ , while depending slightly on  $k_{\max}$ , but our conclusions are not significantly altered as long as  $k_{\max} \gtrsim 0.3 \text{ hMpc}^{-1}$ . It is clear from Figure 1 that the power spectrum is more sensitive to  $\Omega_m$  than  $\bar{w}$ . In our modeling the transfer function depends on  $\Omega_m$ , but not on  $w_X$ . The effect of  $w_X$  on the power spectrum comes from the geometric distortion. The weaker dependence of the power spectrum on  $\bar{w}$  than  $\Omega_m$  originates from this fact.

Figure 2 shows the contour of the marginalized probability function on  $\bar{w} - \nu$  space obtained by integrating (38) with respect to  $(\Omega_m, b_0, p)$ . The target parameters are same as those in Figure 1. Similarly, we set  $z_* = 0.13$  in (40). In this case, it is clear from Figure 2 that the degeneracy between  $\bar{w}$  and  $\nu$  is broken. Note that  $\bar{w} = w_X(z_*)$ . Thus the power spectrum analysis of the LRG sample gives the equation of state around  $z = 0.13$ , almost independently from  $\nu$ . Conversely, the LRG sample is not very sensitive to probe  $\nu$ .

The minimum error in determining the equation of state is  $\Delta\bar{w} \simeq 0.1$ , which is given by integrating the probability function over the other parameters  $(\Omega_m, \nu, b_0, p)$ . The error can be reduced, when  $\Omega_m$  is determined from other observation independently. The result depends on the target parameters. Figure 3 shows the  $1 - \sigma$  error  $\Delta\bar{w}$  as function of  $\Omega_m^{\text{tr}}$ . The solid curves assume  $\bar{w}^{\text{tr}} = -1$ , while the dashed curves assume  $\bar{w}^{\text{tr}} = -0.8$ . The other target parameters are same as those in Figure 1. The error is sensitive to the density parameter  $\Omega_m^{\text{tr}}$ , however, is not sensitive to  $\bar{w}^{\text{tr}}$ . The sensitivity to the equation of state deteriorates in higher matter density universes. This is because the fraction of the dark energy to the total energy decreases as the matter density becomes higher. As long as  $\Omega_m^{\text{tr}} \lesssim 0.3$ , however, the minimum error is  $\Delta\bar{w} \lesssim 0.1$ .

### 3.3. A Luminosity Dependent Bias Model

Here we consider a more realistic bias model. Recent investigations with the 2df galaxy redshift survey report that the clustering amplitude depends on galaxy type and luminosity (Norberg et al. 2001, 2002). The selection effect from an apparent limiting magnitude can have significant influences on the redshift evolution of the bias. Denoting the luminosity dependent bias by  $b(z, L)$ , we define the luminosity-averaged bias as

$$\bar{b}(z) = \frac{\int_{L_{\min}(z)}^{\infty} \phi(L) b(z, L) dL}{\int_{L_{\min}(z)}^{\infty} \phi(L) dL}, \quad (50)$$

---

<sup>2</sup>The dependence on the survey area will be discussed in the final section.

where  $\phi(L)$  is the luminosity function. In modeling  $b(z, L)$ , we assume that  $b(z, L)$  can be approximately written as  $b(z, L) = \hat{b}(z)b(z=0, L)$ . Namely, the luminosity dependence of the bias does not depend on the redshift. Here we also assume  $\hat{b}(z)$  to be described by (cf. Mo & White 1996)

$$\hat{b}(z) = \frac{1}{b_0} \left( 1 + \frac{b_0 - 1}{D(z)} \right), \quad (51)$$

which is normalized to yield 1 at  $z = 0$ , i.e.  $\hat{b}(0) = 1$ . For  $b(z=0, L)$ , we adopt the result by Norberg et al. (2002), who found that the luminosity dependence can be fitted by

$$b(z=0, L) \propto A + (1 - A) \frac{L}{L_*}, \quad (52)$$

where  $A$  is constant. Norberg et al. report  $A = 0.8$  for early-type galaxy (2002). Combining (51) and (52), we assume  $b(z, L)$  can be written in the form

$$b(z, L) = \left( 1 + \frac{b_0 - 1}{D(z)} \right) \left( A + (1 - A) \frac{L}{L_*} \right). \quad (53)$$

Then, expression (50) yields

$$\bar{b}(z) = \left( 1 + \frac{b_0 - 1}{D(z)} \right) \left( A + (1 - A) \frac{\Gamma(\alpha + 2, x(z))}{\Gamma(\alpha + 1, x(z))} \right), \quad (54)$$

where  $\Gamma(\beta, x)$  is the incomplete Gamma function and  $x(z) = L_{\text{lim}}(z)/L_*$ , and we assumed the Schechter luminosity function

$$\phi(L)dL = \phi^* \left( \frac{L}{L_*} \right)^\alpha \exp\left( -\frac{L}{L_*} \right) d\left( \frac{L}{L_*} \right). \quad (55)$$

In the present paper, we adopt the fitting formula for the luminosity function in the reference by Madgwick et al. (2002) for early-type galaxies ( $\alpha = -0.54$  and  $M_* - 5 \log_{10} h = -19.58$ ), and  $m = 19.5$  for the apparent limiting magnitude. Figure 4 shows  $\bar{b}(z)$  as a function of  $z$ , where we set  $b_0 = 1.2$  and  $A = 0.8$ , and we have not considered the luminosity evolution and the k-correction for simplicity.

We consider the bias parameterized by (54) with  $b_0$  and  $A$ , instead of (46) with  $b_0$  and  $p$ , and repeat the evaluation of the Fisher matrix. Here we fix the target parameters,  $\Omega_m = 0.28$ ,  $\bar{w} = -1$  and  $\nu = 0$ . Figure 5 shows the marginalized best statistical error  $\Delta\bar{w}$ , integrating over the parameters except for  $\bar{w}$  as function of the target parameters  $b_0$  with  $A$  fixed  $A = 0.6$  (short-dashed curve),  $A = 0.8$  (solid curve),  $A = 0.9$  (long-dashed curve) and  $A = 1$  (dot-dashed curve). Thus, when the bias evolution can be fitted in the form of (54),  $\Delta\bar{w} \simeq 0.1$ , which is almost the same level as that in Figure 3 for  $A \lesssim 0.9$ . However, for the case  $A = 1$ , the error  $\Delta\bar{w}$  increases out to 0.15, depending on  $b_0$ . This suggests that modeling of the redshift-evolution of the bias can be problematic to constrain the equation of state of dark energy using the LRGs.

#### 4. OPTIMIZED SAMPLE

In this section, we address the problem of determining the optimized sample in order to best constrain the equation of state. This problem might be only of theoretical interest, but having such information could be useful in planning a survey of galaxies or clusters of galaxies. The same problem has been considered with regard to supernova data and lensing systems by several authors (Huterer & Turner 2001, Spergel & Starkman 2002, Yamamoto et al. 2001). To address the problem stated above, we introduce the Fisher matrix element per object as follows: When a survey volume is small enough so that the light-cone (redshift evolution) effect is negligible, (34) is written

$$F_{ij} \simeq \frac{1}{4\pi^2} \int_{k_{\min}}^{k_{\max}} \frac{\Delta V \bar{n}^2}{(1 + \bar{n} P_0(k, s))^2} \frac{\partial P_0(k, s)}{\partial \theta_i} \frac{\partial P_0(k, s)}{\partial \theta_j} k^3 d \ln k, \quad (56)$$

where we assumed  $\bar{n}$  to be constant, and  $\Delta V$  is the survey volume. Then  $F_{ij}/\Delta V$  can be regarded as the Fisher matrix element per unit volume, and similarly  $F_{ij}/(\Delta V \bar{n})$  is regarded as the Fisher matrix element per object. In a strict sense we must choose  $k_{\min}$  and  $k_{\max}$  depending on  $\Delta V$  and  $\bar{n}$ . However, we here fix  $k_{\min} = 0.01 \text{ hMpc}^{-1}$  and  $k_{\max} = 1 \text{ hMpc}^{-1}$ . Then we investigate  $F_{ij}/(\Delta V \bar{n})$  as a function of  $z$  and  $\bar{n}$ . Here note that  $s$  is the function of the redshift, i.e.  $s = s(z)$ .

In this section, for simplicity, we consider the model in which the equation of state is constant  $w_X(z) = \bar{w}$ , which is equivalent to the assumption  $f_X(z) = (1+z)^{3(1+\bar{w})}$ . Regarding the Fisher matrix as the  $2 \times 2$  matrix corresponding to the elements  $\bar{w}$  and  $b_0$ , we consider the marginalized Fisher matrix element integrating the probability function over  $b_0$ :

$$\tilde{F}_{\bar{w}\bar{w}} = F_{\bar{w}\bar{w}} - \frac{F_{\bar{w}b_0}^2}{F_{b_0b_0}}. \quad (57)$$

Figure 6 shows  $[\Delta V \bar{n} / \tilde{F}_{\bar{w}\bar{w}}]^{1/2}$  as a function of  $z$  with  $\bar{n}$  fixed as  $\bar{n} = 10^{-2} \text{ h}^3 \text{Mpc}^{-3}$  (dashed curve),  $10^{-4} \text{ h}^3 \text{Mpc}^{-3}$  (solid curve), and  $10^{-6} \text{ h}^3 \text{Mpc}^{-3}$  (long dashed curve). Figure 6 indicates that objects in the range  $0.4 \lesssim z \lesssim 1$  are most efficient for measuring  $\bar{w}$ , because  $[\Delta V \bar{n} / \tilde{F}_{\bar{w}\bar{w}}]^{1/2}$  is regarded as the error in determining  $\bar{w}$  per object at the redshift  $z$ . Note that the error using the total objects  $\Delta \bar{w}$  scales as  $1/\sqrt{N} = 1/\sqrt{\bar{n} \Delta V}$ . Figure 7 shows  $[\Delta V \bar{n} / \tilde{F}_{\bar{w}\bar{w}}]^{1/2}$  as a function of  $\bar{n}$  with the redshift fixed at  $z = 0.6$ . This figure indicates that the number density around  $\bar{n} = 10^{-4} \text{ h}^3 \text{Mpc}^{-3}$  is most efficient for measuring  $\bar{w}$ . For very sparse samples, like quasars, which have a typical number density  $\bar{n} = 10^{-6} \text{ h}^3 \text{Mpc}^{-3}$ , the errors in measuring parameters using the power spectrum is large due to the shot-noise. On the other hand, for a sample with high number density, the shot-noise is of minor importance, but the efficiency in constraining  $\bar{w}$  per object decreases as well. Thus the objects in the range of redshift  $0.4 \lesssim z \lesssim 1$  with the number density  $\bar{n} \simeq 10^{-4} \text{ h}^3 \text{Mpc}^{-3}$  are the optimized sample.

## 5. CONCLUSIONS

In summary we derived a rigorous optimal weighting scheme for power spectrum analysis, which is useful for samples in which the light-cone effect and the redshift-space distortions are substantial. Our result is a simple extension of the work by FKP, and we obtained a generalized optimal weight factor which minimizes the errors of the power spectrum estimator. As an application of our formula, we investigated the capability of the LRG sample in SDSS to constrain the equation of state parameters by evaluating Fisher matrix elements. Even if the transfer function for the matter power spectrum does not depend on  $w_X$ , the power spectrum analysis of the redshift-space sample can constrain  $w_X$  due to the geometric distortion. To incorporate uncertainties of redshift evolution of the clustering bias, we considered the marginalized probability function by integrating over the parameters of the bias models. This analysis shows that the LRG sample in SDSS has a serviceable potential for constraining the equation of state around  $z = 0.13$  with 1 sigma errors at the 10 % level, if other fundamental parameters are well determined in an independent fashion. We also showed that this conclusion is not altered in the case of a bias model incorporating the redshift-evolution due to selection effect depending on luminosity. However, even in our realistic treatment of the bias, we made simplifications: Uncertainties including the stochasticity and the nonlinearity in modeling the bias are not considered in our investigation. Then, tests on the bias properties will be required for more definite conclusions.

In the present paper, we assumed  $10^4 \text{ deg}^2$  as the complete SDSS survey area. When the planed survey area are not achieved, the capability to constrain the equation of state reduces. As the Fisher matrix element is in proportion to the survey area  $\Delta\Omega$ , then the statistical error  $\Delta\bar{w}$  increases in proportion to  $\sqrt{\Delta\Omega}$ . For example, when we assume  $5 \times 10^3 \text{ deg}^2$  and  $7.5 \times 10^3 \text{ deg}^2$  as the final SDSS survey area,  $\Delta\bar{w}$  increases by 30 % and 15 %, respectively, as long as the inhomogeneity of the incomplete survey area does not cause additional systematic errors.

In section 4, we considered the optimized sample to constrain  $w_X$  using power spectrum analysis. We found that it is most advantageous to have the sample with the comoving number density  $\bar{n} \simeq 10^{-4} h^3 \text{Mpc}^{-3}$  in the range of redshift  $0.4 \lesssim z \lesssim 1$ . For such a sample, the efficiency per object to constrain  $w_X$  is optimized. Information from anisotropic power spectrum would improve the capability of constraining the parameters, as demonstrated in the 2df QSO sample (Outram et al. 2001).

This work was supported by fellowships for Japan Scholar and Researcher Abroad from Japanese Ministry of Education, Culture, Sports, Science and Technology. The author thanks Prof. S. D. M. White for important comments, which helped improve the paper.

Parts of section 3 are based on the valuable communications with him. The author is also grateful to the people at Max-Planck-Institute for Astrophysics (MPA) for their hospitality during his stay. He thanks P. A. Popowski, N. Sugiyama, S. Zaroubi, J. Brinchmann and T. Matsubara for useful discussions and comments. He is also grateful to B. M. Schäfer and K. Basu for reading manuscript and useful comments.

## REFERENCES

- Alcock C., & Paczynski B. 1979, *Nature*, 281, 358
- Bacon D., Massey R., Refregier A., & Ellis R., 2002, astro-ph/0203134
- Ballinger W. E., Peacock J. A., & Heavens A. F. *MNRAS*, 282, 877
- Chiba T., & Nakamura N. 2000, *Phys. Rev. D*, 62, 121301
- de Laix A. A., & Starkmann G. D. 1998, *MNRAS*, 299, 977
- Eisenstein D. J., & Hu W. 1998, *ApJ*, 496, 605
- Eisenstein D. J., et al. 2001, *AJ*, 122, 2267
- Feldman H. A., Kaiser N., & Peacock J. A. 1994, *ApJ*, 426, 23
- Fisher K., Lahav O., Hoffman Y., Lynden-Bell D., & Zaroubi S. 1995, *MNRAS*, 272, 885
- Hamilton A. J. S. 1998, in *The Evolving Universe: Selected Topics on Large-Scale Structure and on the Properties of Galaxies*, ed. D. Hamilton (Dordrecht: Kluwer), 185
- Hoyle F., Outram P. J., Shanks T., Croom S. M., Boyle B. J., Loaring N. S., Miller L. & Smith R. J. 2002, *MNRAS* 329, 336
- Huterer D., & Turner M. S. 2001, *Phys. Rev. D* 64, 123527
- Jungman G., Kamionkowski M., Kosowsky A., & Spergel D. N. 1996a, *Phys. Rev. Lett.*, 76, 1007
- Jungman G., Kamionkowski M., Kosowsky A., & Spergel D. N. 1996b, *Phys. Rev. D* 54, 1332
- Kaiser N. 1987, *MNRAS*, 227, 1
- Kendall M. G., & Stuart A. 1969, *The Advanced Theory of Statistics*, Griffin London
- Kujat J., Linn A. M., Scherrer R. J., & Weinberg D. H. 2002, *ApJ*, 572, 1
- Madgwick S. D., et al. 2002, *MNRAS*, 333, 133
- Magira H., Jing Y. P., Suto Y., 2000, *ApJ*, 528, 30
- Matarrese S., Coles, P., Lucchin F., Moscardini L. 1997, *MNRAS* 286, 115

- Matsubara T., & Suto, Y. 1996, ApJ 470, L1
- Matsubara T., Suto, Y., & Szapudi, I. 1997, ApJ, 491, L1
- Matsubara T., & Szalay A. S. 2002, ApJ, 571, 1
- Matsubara T., & Szalay A. S. 2003, Phys. Rev. Lett. 90, 1302
- Mo H. J., Jing Y. P., & Boerner G. 1997, MNRAS, 286, 979
- Mo H. J., & White S. D. M. 1996, MNRAS, 282, 347
- Neuman J. A., & Davis M. 2000, ApJ, 534, L11
- Norberg P., et al. 2002, MNRAS, 332, 827
- Norberg P., et al. 2001, MNRAS, 328, 64
- Outram P. J., Hoyle F., Shanks T., Boyle B. J., Croom S. M., Loaring N. S., Miller M., & Smith R. J. 2001, MNRAS, 328, 1740
- Peacock J. A., et al. 2001, Nature, 410, 169
- Peebles P. J. E. 1980, *The Large-Scale Structure in the Universe*, Princeton University Press
- Peebles P. J. E., & Ratra B. 2003, Rev. Mod. Phys. 75, 599
- Percival W. J., et al. 2001, MNRAS, 327, 1279
- Perlmutter S., et al. 1999, ApJ, 517, 565
- Refregier A., Rhodes J., & Groth E. J., 2002, ApJ, 572, L131
- Riess A., et al. 1998, AJ, 116, 1009
- Ruhl J. E., et al. 2002, astro-ph/0212229
- Saini T.D., Raychaudhury S., Sahni V., & Starobinsky A. A. 2000, Phys. Rev. Lett., 85, 1162
- Spergel D. N., & Starkman G. D. 2002, astro-ph/0204089
- Spergel D. N., et al. 2003, astro-ph/0302209
- Tegmark M. 1995, ApJ, 455, 429
- Tegmark M. 1997, Phys. Rev. Lett., 79, 3806

- Tegmark M., Eisenstein D. J., Hu W., & Kron R. G. 1998b, astro-ph/9805117
- Tegmark M., Hamilton A. J. S., Vogeley M. A., & Szalay A. S. 1998a, ApJ, 499, 555
- Tegmark M., Taylor A., & Heavens A., 1997, ApJ, 480, 22
- Wang L., Caldwell R. R., Ostriker J. P., & Steinhardt P. J. 2000, ApJ, 530, 17
- Wang L., & Steinhardt P. J. 1998, ApJ, 508, 483
- Watkins R, Feldman H. A., Chambers S. W., Gorman P., and Melott A. L. 2002, ApJ, 564, 534
- Yamamoto K. 2002, MNRAS, 334, 958
- Yamamoto K. 2003, MNRAS, 341, 1199
- Yamamoto K., Kadoya Y., Murata T., & Futamase T. 2001, Prog. Theor. Phys., 106, 917
- Yamamoto K., & Nishioka H. 2001, ApJ, 549, L15
- Yamamoto K., & Suto Y. 1999, ApJ, 517, 1.
- Zaroubi S., Hoffman Y., Fisher K., & Lahav O. 1995, ApJ, 449, 446

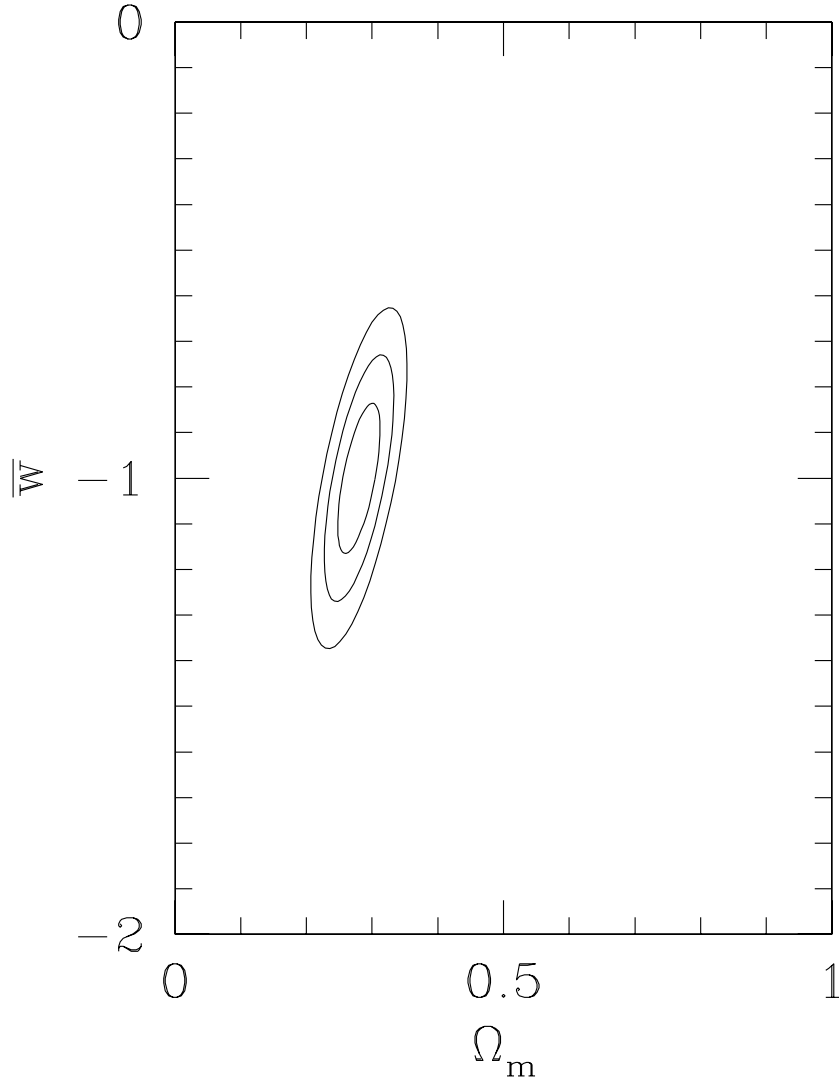


Fig. 1.— Contour of the marginalized probability function in  $\Omega_m$ - $\bar{w}$  space. The curves show 1- $\sigma$ , 2- $\sigma$  and 3- $\sigma$  contours. The target parameters are  $\Omega_m = 0.28$ ,  $\bar{w} = -1$ ,  $\nu = 0$ ,  $b_0 = 1.5$  and  $p = 1$ . In (40) we set  $z_* = 0.13$ . The survey area  $10^4 \text{ deg}^2$  is assumed.

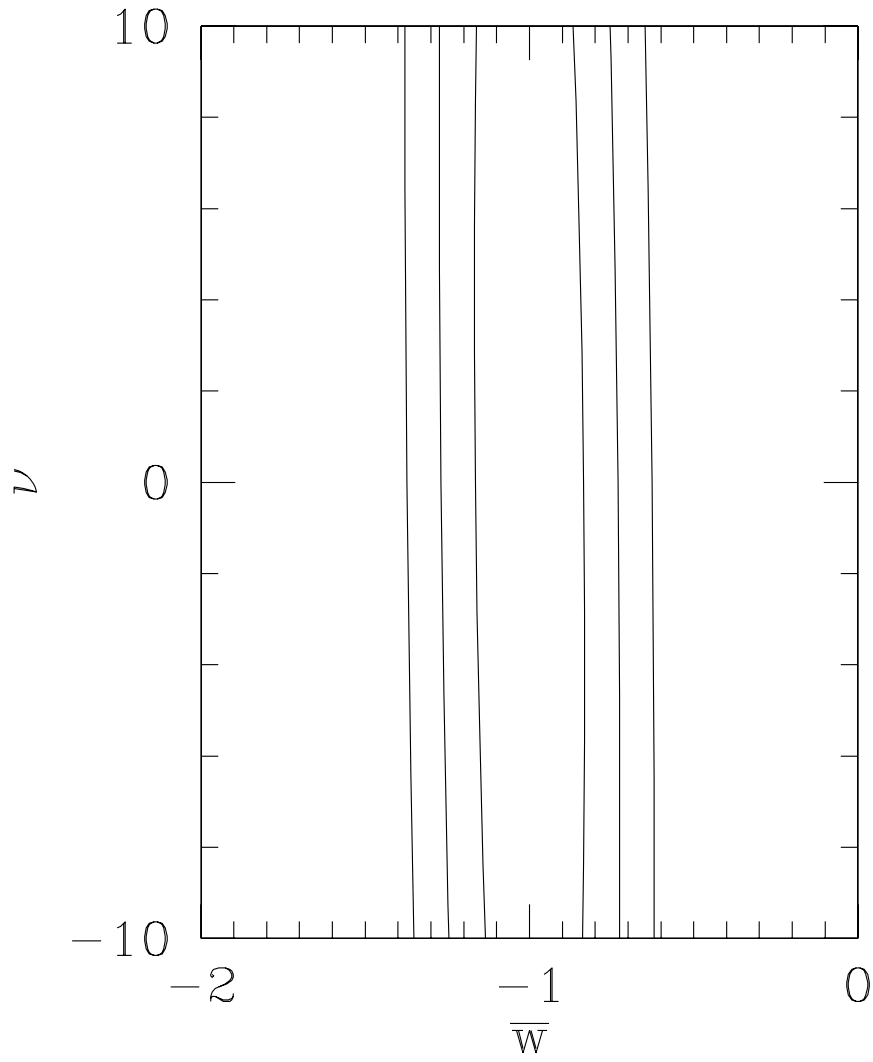


Fig. 2.— Contour of the marginalized probability function in  $\bar{w}$ - $\nu$  space. The meaning of the curves and the parameters are same as those in Figure 1.

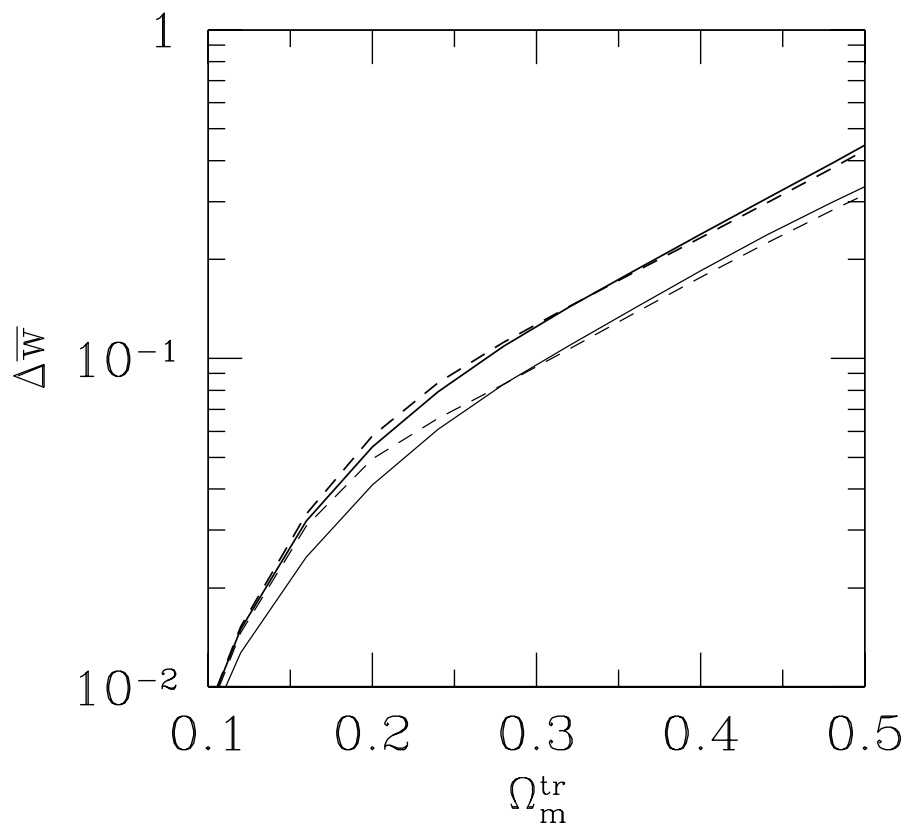


Fig. 3.— The statistical  $1 - \sigma$  error  $\Delta\bar{w}$  as a function of the target parameter  $\Omega_m^{\text{tr}}$ . The solid and dashed curves adopt  $\bar{w}^{\text{tr}} = -1$  and  $\bar{w}^{\text{tr}} = -0.8$ , respectively. For each pair of curves, the lower curve assumes that  $\Omega_m$  is determined by other independent method, while the upper curve assumes that  $\Omega_m$  is determined simultaneously by the power spectrum analysis. The other target parameters are same as those in Figure 1.

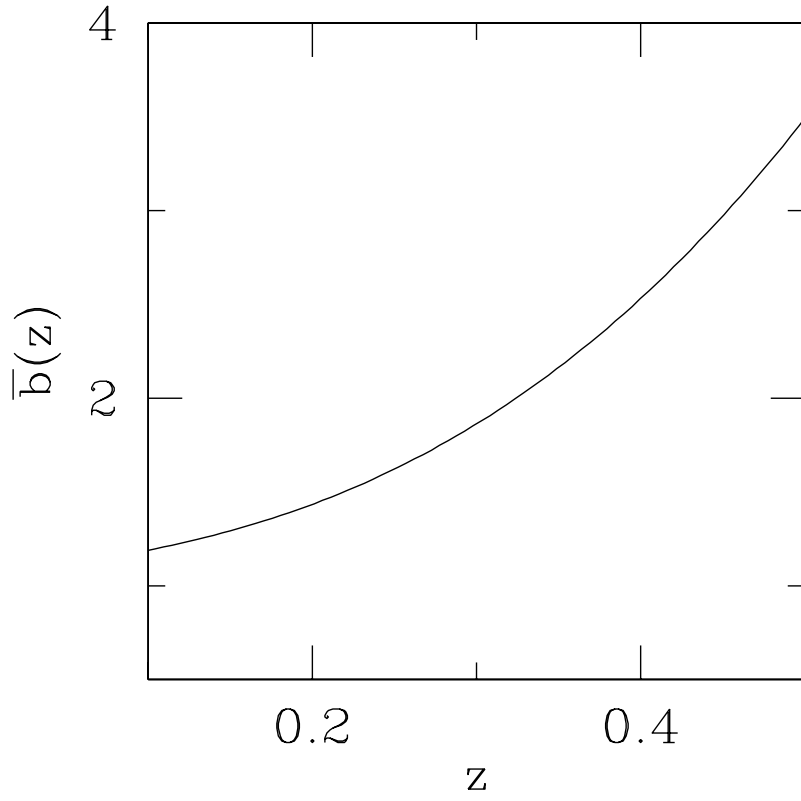


Fig. 4.—  $\bar{b}(z)$  as a function of the redshift. We adopted  $b_0 = 1.2$  and  $A = 0.8$ .

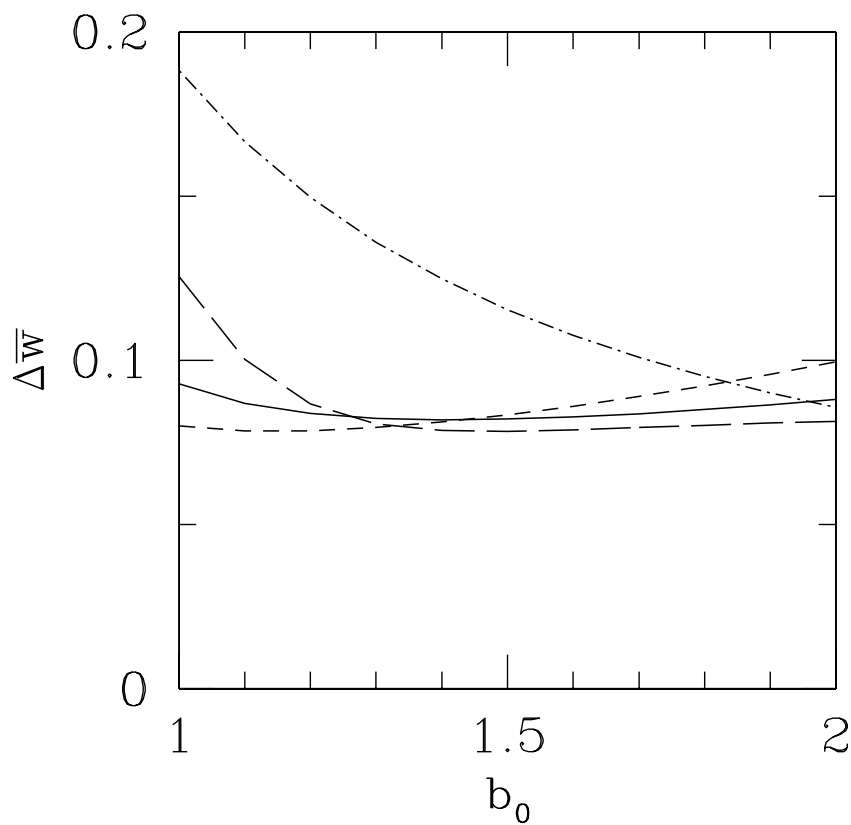


Fig. 5.— The statistical error  $\Delta\bar{w}$  as a function of the target parameter  $b_0$  with fixing  $A = 0.6$  (short-dashed curve),  $A = 0.8$  (solid curve),  $A = 0.9$  (long-dashed curve) and  $A = 1$  (dot-dashed curve) in the bias model in section 3.3. The other target parameters are same as those in Figure 1. Here we assume that  $\Omega_m$  is determined simultaneously by the power spectrum analysis.

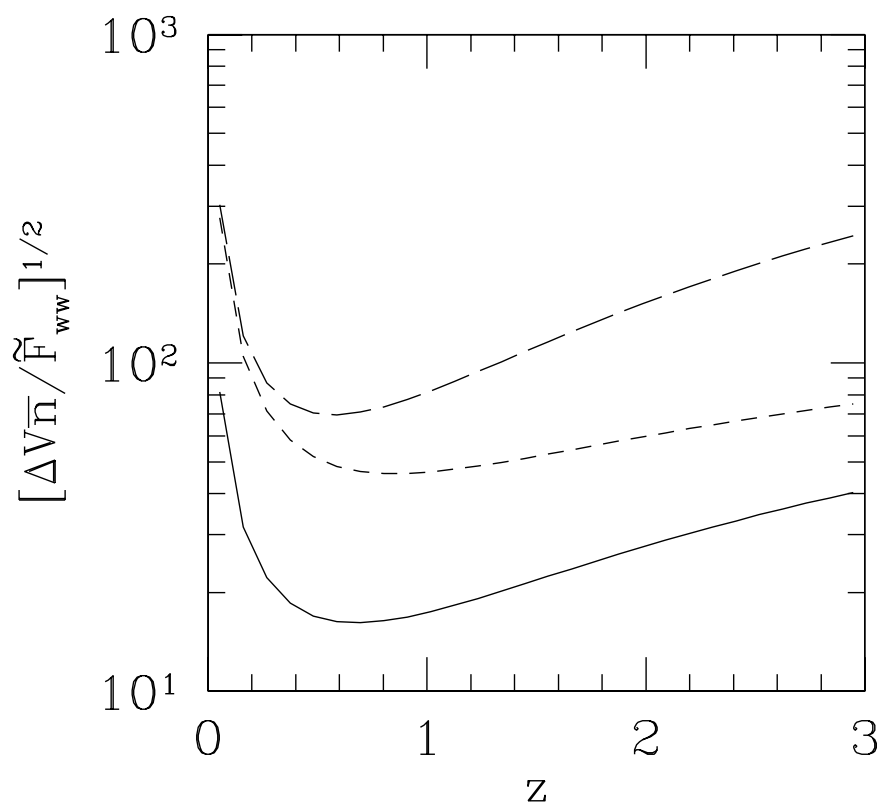


Fig. 6.—  $[\Delta V \bar{n} / \tilde{F}_{\bar{w}\bar{w}}]^{1/2}$  as function of  $z$  with  $\bar{n}$  fixed. The dashed curve, the solid curve, and the long dashed curve, assume  $\bar{n} = 10^{-2} h^3 \text{Mpc}^{-3}$ ,  $10^{-4} h^3 \text{Mpc}^{-3}$ , and  $10^{-6} h^3 \text{Mpc}^{-3}$ , respectively. The target parameters are same as those in Figure 1.

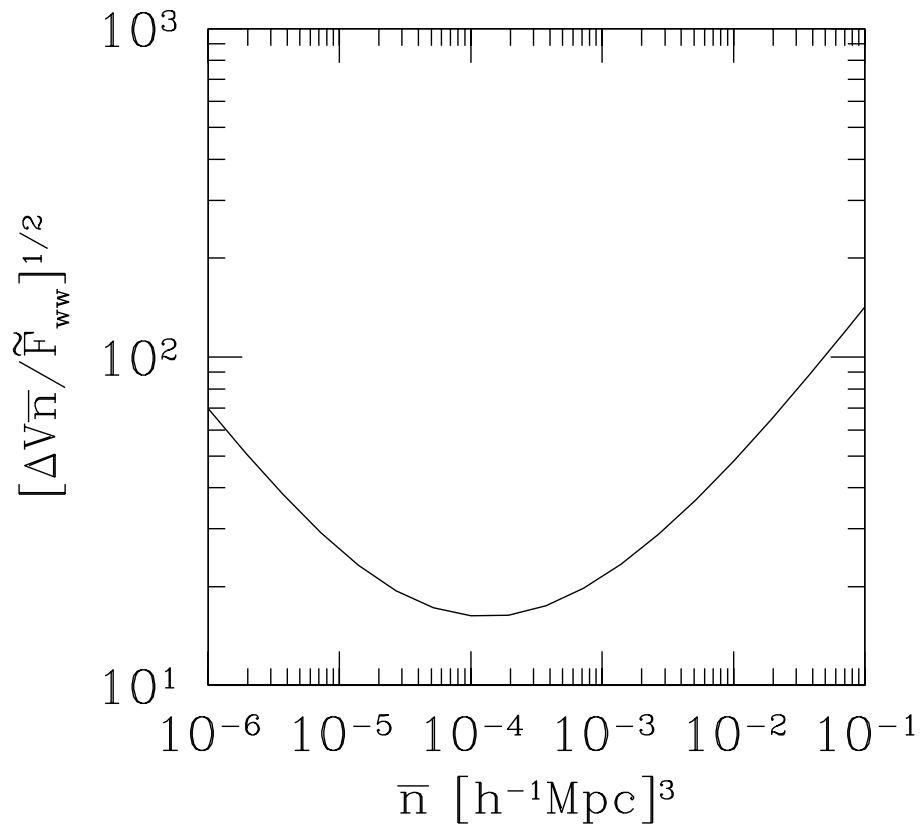


Fig. 7.—  $[\Delta V \bar{n} / \tilde{F}_{w\bar{w}}]^{1/2}$  as a function of  $\bar{n}$ . Here the redshift is fixed at  $z = 0.6$ . The target parameters are same as those in Figure 1.